PROCEEDINGS OF SCIENCE

Annealing studies of irradiated p-type silicon sensors by Edge-TCT*

Gregor Kramberger[†a], **V. Cindro**[a], **I. Mandić**[a], **M. Mikuž**[a,b], **M. Milovanović**[a], **M. Zavrtanik**[a] [‡]

[a] *Jozef Stefan Institute*

[b] *University of Ljubljana, Faculty of Mathematics and Physics, Department of Physics*

E-mail: Gregor.Kramberger@ijs.si

Edge-TCT was used to study avalanche multiplication processes in irradiated p-type silicon micro-strip detectors during long term annealing. The amplification was found to increase with annealing time, but remained moderate. A strong correlation between amplification and leakage current was observed.

19th International Workshop on Vertex Detectors
June 6 -11 2010
Loch Lomond, Scotland, UK

*Work performed in the framework of CERN-RD50 collaboration.

†Speaker.

‡G. Kramberger, V. Cindro, I. Mandić, M. Mikuž, M. Milovanović and M. Zavrtanik are with the Jožef Stefan Institute, Jamova 39, SI-1000 Ljubljana, Slovenia (Tel: (+386) 1 4773512, fax: (+386) 1 4773166,), M. Mikuž is also with University of Ljubljana, Faculty of Mathematics and Physics, Department of Physics, Jadranska 19, SI-1000 Ljubljana.

PoS(VERTEX 2010)021

1. Introduction

Position sensitive silicon detectors are employed at almost all modern high energy physics experiments. Although they are unsurpassed in many aspects of operation, radiation damage appears to be the limiting factor for their operation in the experiments at future colliders. Already at Large Hadron Collider (LHC) the damage of silicon tracking detectors is substantial [1], but the planned future upgrade of LHC luminosity by an order of magnitude [2] poses a serious challenge for successful operation. One of the main problems at LHC is the increase of full depletion voltage (V_{fd}) following long annealing times commonly referred to as reverse annealing. Although the effective doping concentration decreases initially for about 14 days at room temperature after irradiation, it starts to increase again with the time constant of ≈ 1 year at room temperature [1]. As the introduction rate of effective acceptors activated during long term annealing is large ($g_Y \approx 5 \cdot 10^{-2}$ cm^{-2}) the increase of V_{fd} could exceed the power supply limit or break-down voltage already at relatively low fluences of order 10^{14} hadrons cm^{-2}. This was demonstrated for a large number of conventional $p^+ - n$ sensors, where achieving full depletion is crucial, due to the **s**pace **c**harge **s**ign **i**nversion (SCSI) and growth of depletion region from the n^+ back contact. To enable operation with partial depletion $n^+ - n$ detectors were used for the pixel detector layers at LHC. Such detectors have important advantages. The depletion region grows from the segmented electrodes (high weighting field) after SCSI and electrons, which exhibit smaller trapping probability and drift faster, contribute more to the induced charge. In operation terms similar, but less complicated to produce are $n^+ - p$ sensors [3], which are considered as the main candidate for the LHC upgrade. Recently it has been shown that electrons multiply in heavily irradiated sensors under large bias voltages [4, 5, 6, 7, 8, 9]. Moreover, long term annealing was shown not to be harmful to the expected extent for those devices [11] and may even be beneficial [12]. It is the goal of this work to study the impact of annealing on charge collection properties of $n^+ - p$ strip detectors irradiated to high fluence with a new tool, Edge-TCT [5].

2. Experimental procedure

The measurements were performed on a *p*-type micro-strip detector processed by Micron[1] on float zone silicon. The initial resistivity of silicon was around 40 kΩ cm, resulting in full depletion voltage $V_{fd} \approx 16$ V for a 300 μm thick detector. The miniature detector had 1 cm long AC coupled n$^+$ strips with a pitch of 80 μm and implant width of 20 μm (ATLAS geometry). It was irradiated with neutrons in the TRIGA nuclear reactor of the Jožef Stefan Institute in Ljubljana [13, 14] to the equivalent fluence of $\Phi_{eq} = 5 \cdot 10^{15}$ cm^{-2}, corresponding approximately to the benchmark fluence of the ATLAS Insertable B-layer detector [15]. After irradiation the detector was annealed at 60°C in progressive steps to the accumulated time of 10240 min. During each annealing step Edge-TCT measurements were performed at $T = -20^\circ$C. A Peltier element was used for heating and cooling, thus allowing the detector to remain mounted in the setup also during annealing.

The basic principle of the technique is shown in Fig. 1. The narrow laser beam of infrared light ($\lambda = 1054$ nm, 100 ps pulses, 200 Hz repetition rate) illuminates a carefully polished edge of the

[1] Micron Semiconductor Ltd., 1 Royal Buildings, Marlborough Road, Business Park, Lancing Sussex, BN15 8SJ, England

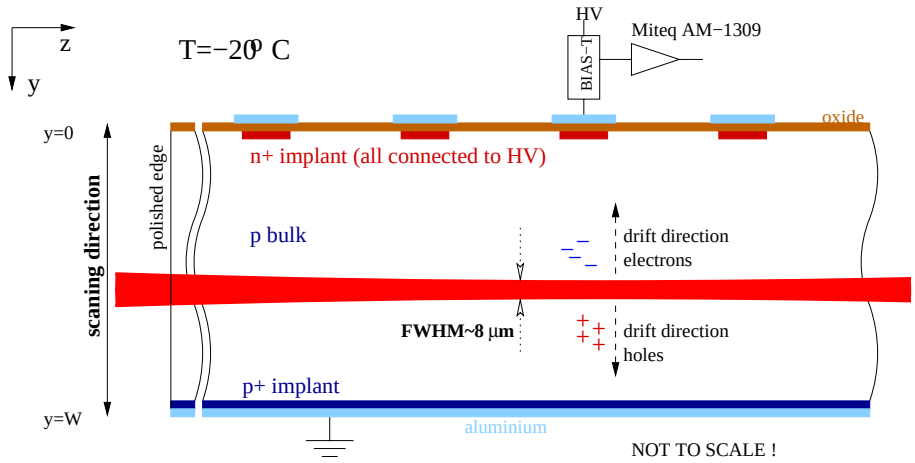

Figure 1: The principle of the experimental technique.

detector. The electron-hole pairs are created almost uniformly along the beam in a similar way as for the minimum ionizing particles. The beam position and by that the depth at which the carriers are generated can be controlled by moving stages with sub-micron precision. In the electric field the carriers start to drift and induce signal in the current amplifier (MITEQ AM-1309, 10 kHz-1 GHz) connected to one of the strips. The average of 400 pulses is taken by a 1.5 GHz oscilloscope at each point. The detailed description of the setup and the measurement technique can be found in Ref. [5].

3. Induced Current Waveforms

The induced current I at the time t after generation of electron-hole pairs at depth y in the detector is given by the equation [5]

$$I(y,t) \;=\; I_e(y,t)+I_h(y,t) \;\approx\; e_0 A N_{e-h}\,\frac{1}{W}\left[v_e(y,t)\,e^{-t/\tau_{eff,e}} \;+\; v_h(y,t)\,e^{-t/\tau_{eff,h}}\right] \quad , \qquad (3.1)$$

where y denotes the beam position, e_0 elementary charge, A amplifier amplification, N_{e-h} number of generated electron hole pairs and $v_{e,h}$ the drift velocities averaged over the strip width at given y. Note that the weighting field term is effectively $1/W$, where W denotes the detector thickness. This is a consequence of uniform generation of charge underneath the strips [5]. The trapping terms become dominant at high fluences [16] and reduces the pulses to ns level.

Two peaks can be observed in the induced current waveforms shown in Fig. 2. The second peak is a consequence of electrons undergoing multiplication upon reaching the high electric field region close to the strips [5]. An increase of the induced current - second peak - is mainly due to drift of holes, produced in multiplication process, towards the p^+ contact ($N_{e-h} = N_{e-h}(y,t) \neq$ const.). At 700 V the electric field is not high enough for a clearly separated second peak to appear after 80 min annealing for any generation depth. At longer annealing times induced current pulses at 50 μm show a “double peak profile” with the second peak becoming the dominant one. This is clearly shown for $y = 150\,\mu$m where the first and the second peak in the induced current are

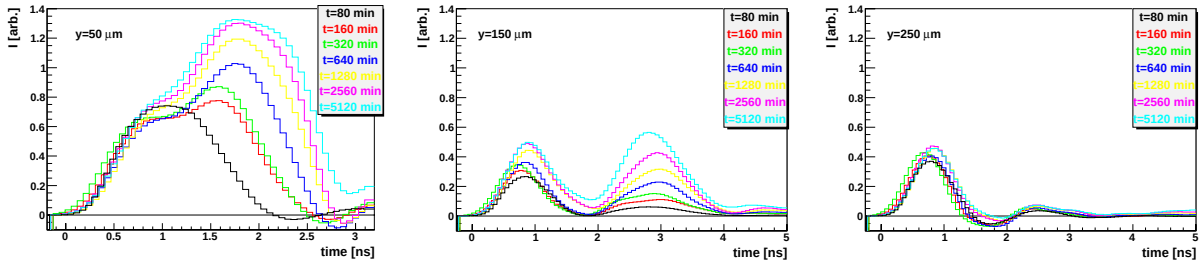

(a) (b) (c)

Figure 2: The induced current waveforms at 700 V during annealing for injection depths: (a) $y = 50\ \mu$m (b) $y = 150\ \mu$m and (c) $y = 250\ \mu$m.

well separated in time. There are two reasons for that. The main reason is the increase of the electric field close to the strips with long term annealing as the effective acceptors are introduced [1]. The long term annealing also reduces the effective trapping probability of electrons therefore more electrons reach the multiplication region.

The first peak amplitude which is associated with the initial drift of primarily generated carriers (primary peak) remains similar at all annealing times. This is an indication that the drift velocity does not change much with annealing and that it is already in the saturation regime. For the carries generated at the back of the detector ($y = 250\ \mu$m) only the primary peak can be seen as the amount of electrons reaching the strips is too small, due to the trapping distance $\lambda_e = v_e\,\tau_{eff,e} \leq 70\ \mu$m.

The importance of applying high bias voltage can be seen in Fig. 3. As can be seen close to the strips the electric field at 400 V is already strong enough for avalanche multiplication. At 50 μm the multiplied charge dominates over the primary charge already at 500 V. At 150 μm the multiplied charge becomes significant at 600 V and becomes dominant for $V_{bias} \geq 800$ V. No charge coming from the multiplication process can be observed for primary carriers generated at $y = 250\mu$m. As expected the bias voltage has a significant impact on the induced charge originating from the drift of the primarily generated carriers, particularly at lower voltages.

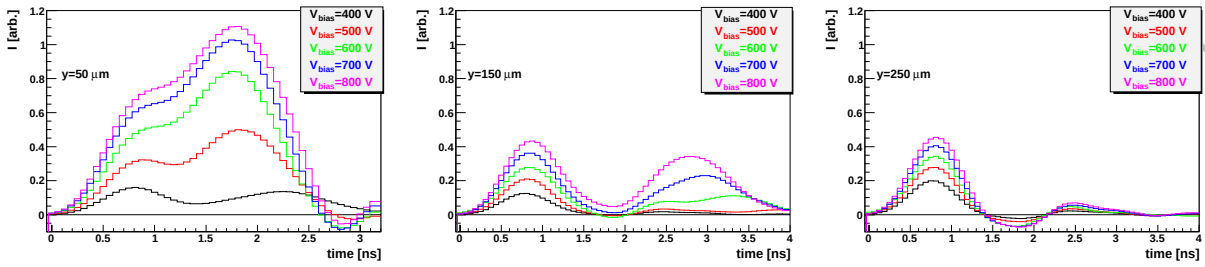

(a) (b) (c)

Figure 3: The induced current waveforms at different bias voltages after 640 min annealing at 60 °C for injection depths: (a) $y = 50\ \mu$m, (b) $y = 150\ \mu$m and (c) $y = 250\ \mu$m.

4. Charge collection and multiplication profiles

An Edge-TCT scan allows for a determination of the charge collection profile $Q(y) = \int_0^{25\text{ ns}} I(y,t)\,dt$ which identifies the regions of high and low charge collection efficiency. The profiles for the inves-

tigated detector at different annealing times are shown in Fig. 4a. It is evident that the collection efficiency is higher at the strip side. The annealing has a beneficial effect and $Q(y)$ increases while the shape remains the same.

In order to enable a relative comparison of $Q(y)$ at different annealing times the samples were annealed at 60°C while being mounted in the measurement setup. This also ensured that the same spot of the detector was illuminated and hence the influence of geometry could be excluded. The

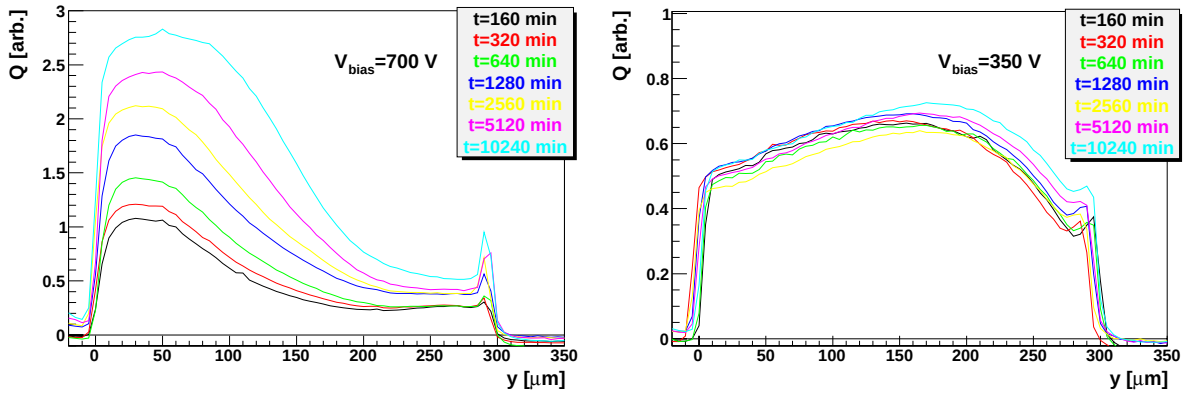

(a) (b)

Figure 4: Charge collection profiles at different annealing times biased to : (a) 700 V in reverse direction and (b) 350 V in forward direction.

stability of the laser was checked by measurements of charge collection profile with the detector biased in the forward direction and can be seen in Fig. 4b. It is evident that when the detector is operated in the forward direction annealing has almost no effect, which is turn confirms that the intensity of the laser was stable.

Unlike in the reverse direction $Q(y)$ in the forward direction has a maximum close to the centre of the detector ($y_{max} \approx 180\ \mu$m) and is determined by the trapping distances of electrons and holes. Maximum charge is induced for $W - y_{max} > \lambda_e$ and $y_{max} > \lambda_h$, with bias voltage determining the precise value. Such a shape is therefore in agreement with a moderate electric field profile $E \propto \sqrt{\frac{y}{W}}$ [17]. It is also interesting to note that also under forward bias the electrons exhibit a smaller trapping probability than holes. Even when the electrons were injected at the low field side ($y \sim 0$) and holes at the high field side ($y \sim W$) the induced charge $Q(y \to 0) > Q(y \to W)$.

The induced charge corresponding to the one induced by a minimum ionizing particle can be estimated as $Q_{mip} \propto < Q > = \int_0^W Q(y)\, dy$ and is shown in Fig. 5. Two regions can be identified. At lower voltages, before the onset of amplification, $< Q >$ rises slowly. Once the field is high enough the $< Q >$ increases at larger rate with bias voltage. However, operation in the forward bias mode at given voltage and higher leakage current yields more charge, except at the last annealing steps. In both bias directions no saturation of the induced charge can be observed. It should be mentioned that the increase of $< Q >$ during the long term annealing is significantly larger than expected from the measurements with electrons from ^{90}Sr source [12, 18], however for different detectors. The reason is not yet clear.

The charge collection profile can be split into contribution from primarily generated e-h pairs and multiplied carriers. At large enough y, both waveform peaks can be clearly separated as shown

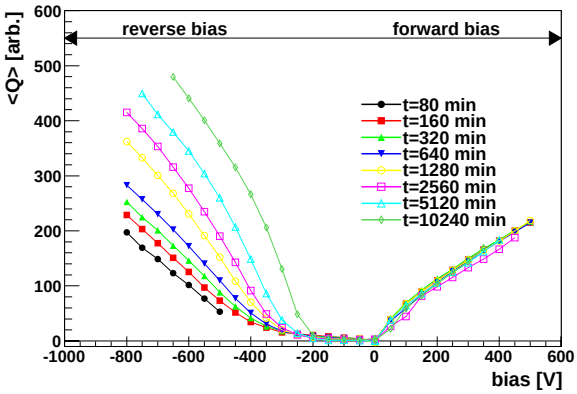

Figure 5: $< Q >$ dependence on bias voltage at different annealing times for both forward and reverse bias.

for example in Fig. 2b for $y = 150\mu$m. At smaller y the pulses begin to overlap, but for $y \gtrsim 70-80$ μm the saddle point can still be determined. The induced current integral - charge Q_{prim} - up to the saddle point ($t_{sad} = 1.9$ ns in Fig. 2b) is attributed to the drift of primarily generated carriers, while the one for $t > t_{sad}$ is due to multiplied charges. As the pulses overlap it is not possible to separate the falling part of the first pulse and the rising part of the second. With a rough approximation that they are equal the multiplication profiles at different annealing times could be obtained (see Fig. 6a). As can be seen the primary charge (blue markers) is almost independent on annealing time, while the induced charge coming from the amplification (red markers) increases with annealing time. On the other hand the bias voltage influences both primary and to larger extent the multiplied charge as shown in Fig. 6b.

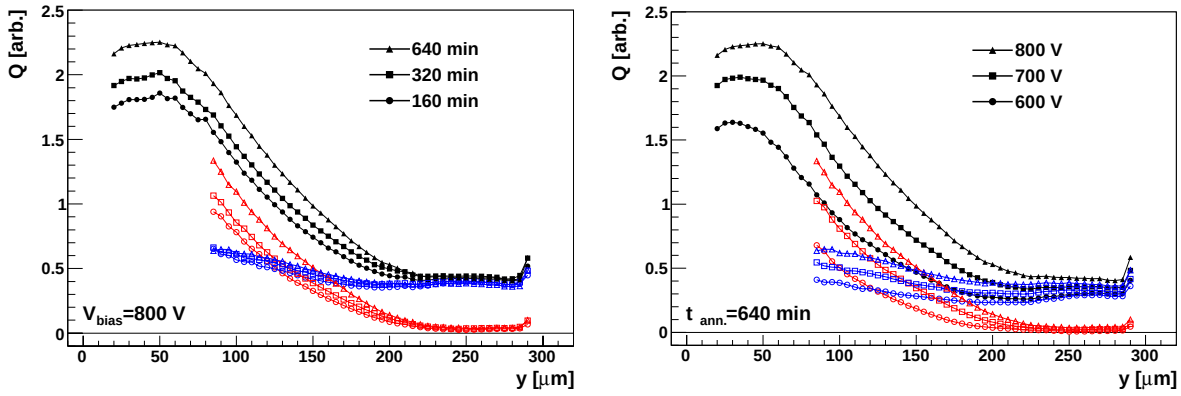

(a) (b)

Figure 6: Charge collection profile (black markers) split into both contributions; primary charge (blue) and multiplied charge (red): (a) for different annealing times at 800 V and (b) for different bias voltages after 640 min annealing.

Although the amplification factor M_Q given by

$$M_Q = \frac{\int_o^W Q(y)\,dy}{\int_o^W Q_{prim}(y)\,dy} \quad , \tag{4.1}$$

cannot be calculated without knowing $Q_{prim}(y < 80\mu\text{m})$, it is reasonable to assume that the velocity is close to saturation and the $Q_{prim}(y < 80\mu\text{m})$ remains close to that at $\approx 80\ \mu$m. In such a way calculated multiplication factors for the profiles shown in Figs. 6 are moderate $M_q \approx 2-3$. Unlike in proportional wire chambers where the multiplication factor increases rapidly with bias voltage, the increase of the bias voltage by few hundred volts results only in a small increase of M_Q. Possible explanation would be that holes produced in multiplication of thermally generated carriers are trapped and by that reduce the negative space charge and thus the peak electric field. This reasoning would still need to be confirmed by simulations.

5. Leakage current and multiplication

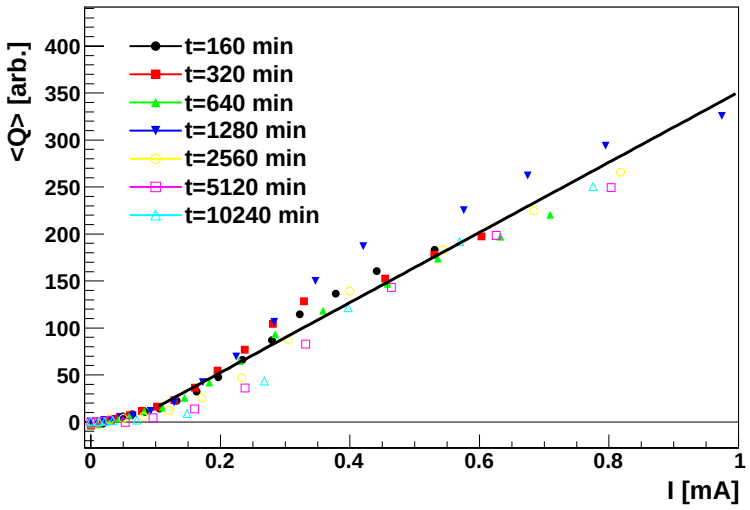

Figure 7: Correlation of measured $< Q >$ and I_{meas} at different annealing times for applied bias voltages.

Thermally generated carriers which give rise to the leakage current also undergo multiplication. Therefore the leakage current is no longer given only by the generation volume, but also depends on the applied bias. The multiplication factor should therefore be correlated with the leakage current. The correlation between the measured charge and the leakage current at different bias voltages and annealing times is shown in Fig. 7. The expected leakage current for a detector with the electric field established in the whole volume at $T = -20^{\circ}$C is around $I_{vol} \approx 0.1$ mA after 160 min annealing. Given that the setup allowed only for the measurement of the sum of bulk and guard ring currents the uncertainty in the current is large. In spite of that it is clear that the current multiplication factor defined by $M_I = I_{meas}/I_{vol}$ is different that of the charge M_Q. For example, $M_Q \approx 2.5$ (see Fig. 6a) at 640 min and 800 V, while $M_I \sim 7$. In a steady state as many carriers are trapped as de-trapped and, if recombination is not significant, every electron eventually undergoes multiplication at the strip. M_I therefore denotes how many carriers are produced from a single electron. Only in absence of trapping and recombination $M_I = M_Q$ would hold, hence $M_I > M_Q$.

6. Discussion

In trackers most charged particles traverse detectors close to perpendicular to the detector surface, hitting few strips/pixels at most. If these are connected to separate amplifiers, the induced charge in each differs from $< Q >$, because the weighting field in Edge-TCT is effectively the same as in a diode. The carriers drifting over the same distance close to the strips and at the back contribute differently due to the weighting field in a strip detector. This is beneficial since the multiplied holes drifting close to strips induce more charge before being trapped than they do in Edge-TCT. The multiplication factor for a minimum ionizing particle $M_{Q,mip}$ hitting a single strip/pixel should therefore be larger than M_Q with the upper limit set by M_I.

An increase of leakage current results in increase of the noise, which can reduce or even diminish the gain in signal-to-noise ratio. The equivalent noise charge of a preamplifier-shaping amplifier circuitry connected to the electrode can be split into serial/voltage (ENC_s) and parallel/current (ENC_p) noise, which add in squares $ENC^2 = ENC_p^2 + ENC_s^2$. The parallel noise for irradiated detectors is dominated by the shot noise while the serial noise depends on the amplifier design and detector capacitance. The shot noise contribution in the multiplication mode of operation is given by [19]

$$ENC_{MI} \approx ENC_I \cdot \sqrt{F} \cdot M_I \quad , \tag{6.1}$$

where ENC_I denotes the shot noise due to bulk current without amplification and F the excess noise factor $F(M >> 1) \approx 2$, $F(M = 1) = 1$. The fact that $M_I \geq M_Q, M_{Q,mip}$ means that for a beneficial effect of multiplication the series noise should dominate over the parallel noise otherwise the signal-to-noise ratio will decrease with multiplication. Amplification mode of operation is therefore appropriate for finely segmented structures (pixels/strips) operated at temperatures, where ENC_I can be kept sufficiently low. Since the M_I can be controlled by the bias voltage there should be an optimum bias voltage for a particular device at each fluence.

7. Conclusions

The measurements have revealed that long term annealing is beneficial in terms of charge collection efficiency of a heavily irradiated $n^+ - p$ silicon strip detectors when operated under reverse bias. Under forward bias the annealing has no impact on the charge collection profile nor collected charge. The use of Edge-TCT technique enabled a separation of induced charge originating from primarily generated carriers and that from multiplied carriers. As expected the multiplied charge starts to dominate at depths of 100 μm. The estimated multiplication factors for ionizing particle tracks perpendicular to the surface were moderate, around 2-3 for bias voltages up to 800 V. Collected charge was found to be reasonably correlated with leakage current, irrespectively of the the annealing stage and bias voltage. On the other hand the multiplication factor for the leakage current was much larger than that for the average charge collection.

References

[1] G. Lindström et al., "Radiation hard silicon detectors - developments by the RD48 (ROSE) collaboration", Nucl. Instr. and Meth. A 466 (2001) p. 308.

[2] F. Gianotti et al., hep-ph/0204087, 2002.

[3] G. Casse et al.,"First results on the charge collection properties of segmented detectors made with p-type bulk silicon", Nucl. Instr. and Meth. A 487 (2002) p. 465.

[4] I. Mandić et al.,"Measurement of anomalously high charge collection efficiency in n^+-p strip detectors irradiated by up to 10^{16} n_{eq}/cm^2, Nucl. Instr. and Meth. A 603 (2009) p. 263.

[5] G. Kramberger et al.,"Investigation of irradiated silicon detectors by Edge-TCT", IEEE Trans. Nucl. Sci. Vol. 57(4), 2010, p. 2294.

[6] G. Casse et al., "Can we claim charge multiplication in heavily irradiated segmented detectors?", presented at 14^{th} RD-50 Workshop, Freiburg, Germany, 2009.

[7] J. Lange et al.,"Detailed investigation of charge multiplication properties in highly irradiated thin epitaxial silicon diodes", presented at 15^{th} RD-50 Workshop, CERN, Geneve, Switzerland, 2009.

[8] J. Lange et al.,"Charge Multiplication Properties in Highly Irradiated Epitaxial Silicon Detectors", these proceedings.

[9] M. Köhler et al., "Beam Test Measurements With Irradiated 3D-DDTC Silicon Strip Detectors", presented at 5^{th} Workshop on 3D and p-type sensors, Manchester, UK, 2010.

[10] R. Bates et al.,"Irradiation studies of CNM double sided 3D detectors", presented at 5^{th} Workshop on 3D and p-type sensors, Manchester, UK, 2010.

[11] P.P. Allport et al.,"Performance of P-Type Micro-Strip Detectors After Irradiation to $7.5 \cdot 10^{15}$ p cm^{-2}", IEEE Trans. Nucl. Sci. 52(5) (2005) p. 1903.

[12] I. Mandić et al.,"Annealing effects in irradiated HPK strip detectors measured with SCT128 chip", presented at 16^{th} RD-50 Workshop, Barcelona, Spain, 2010.

[13] M. Ravnik and R. Jeraj, "Research reactor benchmarks", Nucl. Sci. Eng. Vol. 145 (2003) p. 145.

[14] D. Žontar, V. Cindro V, G. Kramberger, M. Mikuž, "Time development and flux dependence of neutron-irradiation induced defects in silicon pad detectors", Nucl. Instr. and Meth. A 426 (1999) p. 51.

[15] ATLAS-IBL Tecnical Design Report, in preparation (EDMS document ATU-GE-MN-0030 v.15).

[16] G. Kramberger , V. Cindro, I. Mandić, M. Mikuž, M. Zavrtanik, "Effective trapping time of electrons and holes in different silicon materials irradiated with neutrons, protons and pions", Nucl. Instr. and Meth. A 481 (2002) p. 297.

[17] V. Eremin et al., "The operation and performance of Current Injected Detector (CID)", Nucl. Instr. and Meth. A 581 (2007) p. 356.

[18] G. Casse et al.,"Update on Annealing Studies for Severely Irradiated Silicon Detectors", presented at 5^{th} Workshop on 3D and p-type sensors, Manchester, UK, 2010.

[19] P. P. Webb et al., RCA Review 35 (1974) 234.